Journal of Protein Chemistry, Vol. 21, No. 6, August 2002 (© 2002)

Activation of Dynamin II by POPC in Giant Unilamellar Vesicles: A Two-Photon Fluorescence Microscopy Study

L. A. Bagatolli,[1] D. D. Binns,[2] D. M. Jameson,[3] and J. P. Albanesi[2,4]

Received April 12, 2002

The interaction of dynamin II with giant unilamellar vesicles was studied using two-photon fluorescence microscopy. Dynamin II, labeled with fluorescein, was injected into a microscope chamber containing giant unilamellar vesicles, which were composed of either pure 1-palmitoyl-2-oleoyl-sn-glycero-3-phosphocholine (POPC) or a mixture of POPC and phosphatidylinositol 4,5-bisphosphate ($PI(4,5)P_2$). Binding of the fluorescent dynamin II to giant unilamellar vesicles, in the presence and absence of $PI(4,5)P_2$, was directly observed using two-photon fluorescence microscopy. This binding was also visualized using the fluorescent *N*-methylanthraniloyl guanosine 5′-[γ-thio]triphosphate analogue. The membrane probe 6-dodecanoyl-2-dimethylamine-naphthalene was used to monitor the physical state of the lipid in the giant unilamellar vesicles in the absence and presence of dynamin. A surprising finding was the fact that dynamin II bound to vesicles in the absence of $PI(4,5)P_2$. Activation of the GTPase activity of dynamin II by pure POPC was then shown.

KEY WORDS: Dynamin; fluorescence; giant unilamellar vesicles; 1-palmitoyl-2-oleoyl-sn-glycero-3-phosphocholine (POPC); *N*-methylanthraniloyl guanosine 5′-[γ-thio]triphosphate (mant-GTPγS); two-photon microscopy.

1. INTRODUCTION

Dynamins are closely related GTPases[5] of ~100,000 MW that are essential for receptor-mediated endocytosis and synaptic vesicle recycling (reviewed in Hinshaw, 1999; McNiven, 1998; Schmid *et al.*, 1998; van der Bliek, 1999a, 1999b) and that have been implicated in Golgi (McNiven *et al.*, 2000; Jones *et al.*, 1998; Cao *et al.*, 1998) and caveolar trafficking (Henley *et al.*, 1998; Oh *et al.*, 1998). Two forms of dynamin have been extensively characterized: a neuron-specific form called *dynamin I* and a ubiquitously expressed form called *dynamin II*. In neurons, which contain both forms of the enzyme, dynamin I is expressed at ~10-fold higher levels than is dynamin II. These two proteins have a similar organization of functional domains (Fig. 1). These domains include an N-terminal GTPase domain (residues 1–300), a pleckstrin-homology (PH) domain that interacts with phosphatidylinositol lipids (residues 510–620) (Zheng *et al.*, 1996; Salim *et al.*, 1996), a GTPase effector domain that stimulates dynamin GTPase activity (residues 620–750) (Muhlberg *et al.*, 1997), and a C-terminal proline-arginine–rich domain that targets dynamin to the clathrin-coated pit (Okamoto *et al.*, 1997; Shpetner *et al.*, 1996) and binds to a subset of src-homology-3-domain–containing proteins (reviewed in McPherson, 1999), negatively charged phospholipids (Tuma *et al.*, 1993), and microtubules (Shpetner and Vallee, 1992). The self-association modes of dynamins I and II and their mechanisms of GTP hydrolysis have been investigated using ultracentrifugation and stopped-flow fluorescence techniques (Binns *et al.*, 1999, 2000).

[1] Grupo de Biofisica, Dpto. de Química Biológica, Fac. de Ciencias Químicas, UNC, Pabellón Argentina, Ciudad Universitaria, 5000, Córdoba, Argentina.

[2] Department of Pharmacology, University of Texas, Southwestern Medical Center, Dallas, Texas 75235-9041.

[3] Department of Cell and Molecular Biology, University of Hawaii, Honolulu, Hawaii 96822.

[4] To whom correspondence should be addressed. Tel: 214-648-3200; Fax: 214-648-2971; E-mail: Joseph.Albanesi@UTSouthwester.edu

[5] Abbreviations: GP, generalized polarization; GTP, guanosine 5′-triphosphate; GTPγS, guanosine 5′-[γ-thio]triphosphate; GUV, giant unilamellar vesicles; LAURDAN, 6-dodecanoyl-2-dimethylamine-naphthalene; mant, *N*-methylanthraniloyl; PC, phosphatidylcholine; PH, pleckstrin homology; PI(4)P, phosphatidylinositol 4-phosphate; $PI(3,4,5)P_3$, phosphatidylinositol (3,4,5)-trisphosphate; $PI(4,5)P_2$, phosphatidylinositol (4,5)-bisphosphate; POPC, 1-palmitoyl-2-oleoyl-sn-glycero-3-phosphocholine.

0277-8033/02/0800-0383/0

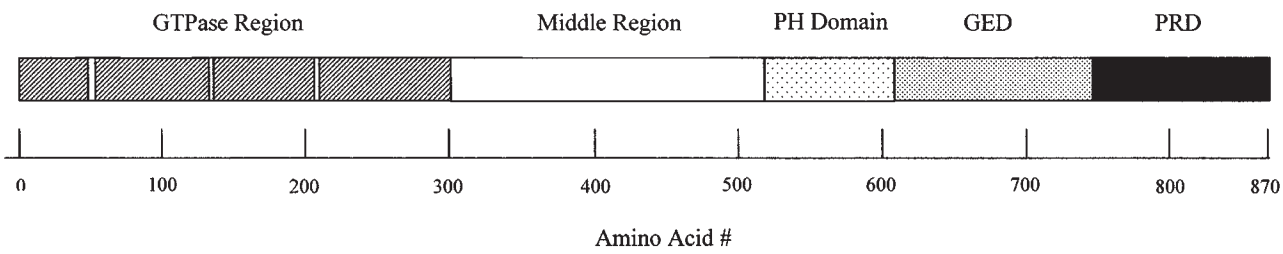

Fig. 1. Schematic diagram of the functional domains of dynamin.

Using fluorescence spectroscopy, Zheng *et al.* (1996) determined that phosphatidylinositol 4-phosphate (PI(4)P), phosphatidylinositol (4,5)-bisphosphate (PI(4,5)P_2), phosphatidylserine, and phosphatidylcholine (PC) bind to the PH domain of dynamin with equilibrium dissociation constants of 1.8, 4.4, 47, and >250 μM, respectively. Using surface plasmon resonance, Salim *et al.* (1996) found that the strength of binding of phospholipids to the PH domain of dynamin was PI(4,5)P_2 > PI(4)P > phosphatidylinositol (3,4,5)-trisphosphate (PI(3,4,5)P_3). Salim and coauthors also found that PC did not bind at all to the PH domain of dynamin. However, when considering the ability of various phospholipids to stimulate the GTPase activity of full-length bovine brain dynamin I, Barylko *et al.* (1998) found that PC vesicles containing PI(4,5)P_2 were more potent activators of dynamin GTPase activity than vesicles containing PI(3,4,5)P_3, which were, in turn, more potent activators than vesicles containing PI(4)P. PC vesicles by themselves have not been found to stimulate the activity of dynamin I, and phosphatidylserine vesicles activate dynamin through the proline-arginine–rich domain (Tuma *et al.*, 1993).

To directly investigate the interaction of dynamin with lipids, we used the approach of two-photon fluorescence microscopy coupled with giant unilamellar vesicles (GUVs). Simplified lipid systems, such as vesicles and micelles, have been studied for several decades as model membranes (Gennis, 1989). These vesicles may vary in size (e.g., 100–800 nm in diameter) and heterogeneity (e.g., unilamellar or multilamellar). Recently, GUVs have been prepared by the method of electroformation (Angelova *et al.*, 1992). The fact that the GUVs are of the same size as many cells (~5–100 μ) and that single vesicles can be directly observed under the microscope has led to an expanding interest in GUVs as model membrane systems. During the last decade, the technique of multiphoton spectroscopy–microscopy has been increasingly applied to lipid systems (Parasassi *et al.*, 1997; Yu *et al.*, 1996; Bagatolli and Gratton, 1999, 2000a, 2000b, 2001; Bagatolli *et al.*, 2000; Dietrich *et al.*, 2001). The combination of GUVs and two-photon fluorescence microscopy has proven to be a powerful approach for understanding lipid dynamics. Specifically, the intrinsic sectioning effect of two-photon microscopy, in combination with the photophysical properties of the membrane probe 6-dodecanoyl-2-dimethylamine-naphthalene (LAURDAN), has been used to detect and quantify lipid domains in GUVs composed of various lipid mixtures (Bagatolli and Gratton, 1999, 2000a, 2000b, 2001; Dietrich *et al.*, 2001; Bagatolli *et al.*, 2000, 2001). Until now, the application of GUVs and two-photon fluorescence microscopy has been largely restricted to GUVs containing only lipids. Recently, we extended these studies to observe the interaction of a lipid-binding protein, dynamin, with GUVs.

Lin *et al.* (1997) also showed that dynamin II, purified from overexpressing *Spodoptera frugiperda* cells, behaved similarly to dynamin I in terms of its activation by phosphoinositides. Due to the ease in obtaining large quantities of this recombinant enzyme, we decided to initiate our investigation of dynamin–GUV interactions using dynamin II rather than dynamin I. Moreover, although dynamin II is expected to affect membrane morphology similarly to dynamin I given the percentage of sequence identity between the two proteins, no reports have appeared to show this similarity in function directly using a simple reconstituted system. A surprising outcome of this research, described subsequently, was the finding that dynamin II not only binds to pure PC vesicles but, unlike dynamin I, is enzymatically activated by that neutral lipid. This result raises the possibility that dynamins I and II, which participate in synaptic vesicle recycling and receptor-mediated endocytosis, respectively, may be subject to different modes of regulation.

2. MATERIALS AND METHODS

2.1. Materials

LAURDAN and 5-iodoacetamidofluorescein were from Molecular Probes (Eugene, OR). 1-Palmitoyl-2-oleoyl-sn-glycero-3-phosphocholine (POPC) and PI(4,

5)P_2 were from Avanti Polar Lipids (Alabaster, AL). Phospholipids were used without further purification. *N*-Methylanthraniloyl guanosine 5′-[γ-thio]triphosphate (mant-GTPγS) (mant-GTPγS) was synthesized and purified according to previously described methods (Remmers, 1998; Jameson and Eccleston, 1997).

2.2. Dynamin Preparation and Labeling

Dynamin II was obtained as described previously (Lin *et al.,* 1997). For protein labeling, 20 μl of a 20-mM solution of 5-iodoacetamidofluorescein in *N*,*N*′-dimethylformamide was added to 1.0 ml of 20-μM dynamin II in buffer [20 mM *N*-(2-hydroxyethyl)piperazine-*N*′-(2-ethanesulfonic acid), pH 7.4; 300 mM NaCl; 5 mM $MgCl_2$; 1 mM ethylenediamine tetraacetic acid; and 0.2 mM phenylmethanesulfonyl fluoride]. The mixture was incubated in the dark at 4°C for 8 hr. After the incubation dithiothreitol was added to the mixture (final dithiothreitol concentration, 5 mM) and a 30-column Bio-Rad Econopak was used to exchange the buffer. The fluorescein-labeled protein was then dialyzed against the same buffer to remove any residual free dye. The protein concentration was determined by Bradford assay against a bovine serum albumin standard. The absorbance of the 5-iodoacetamidofluorescein–labeled dynamin II was measured at 492 nm, and the protein concentration was determined using an extinction coefficient of 75,500 cm^{-1} M^{-1} at this wavelength. The dye to protein ratio was determined to be ~2.

2.3. GUV Preparation

The GUVs were prepared using the electroformation method (Angelova *et al.,* 1992) in a homemade chamber (see Fig. 2). Stock solutions of phospholipids were made in chloroform (lipid final concentration, 0.2 mg/ml). The following steps were used for vesicle preparation: (1) ~5 μl of lipid stock solution were spread (pure POPC or POPC/PI(4,5)P_2,10:1 mol/mol) on each Pt wire under a stream of N_2. The chamber was placed in a lyophilizer for 2 hr to remove the organic solvent residues from the Pt wires; (2) the bottom part of the chamber was sealed with a coverslip, and the chamber was placed on an inverted microscope (Axiovert 35, Zeiss, Thornwood, NY); and (3) Millipore water (17.5 MΩ/cm) at room temperature was added to the chamber covering the Pt wires. The Pt wires were then immediately connected to a function generator (Hewlett-Packard, Santa Clara, CA) for ~90 min and a low-frequency alternating current (AC) field (sinusoidal wave function with a frequency of 10 Hz and an amplitude of 2 V) was applied. The vesicle formation was followed using a CCD color video camera (CCD-Iris, Sony) mounted on the side port of the microscope (Fig. 2). After 70 min, large numbers of vesicles (vesicle mean diameter, ~30 μm) were observed adsorbed to the Pt wire. The unilamellar vesicle yield was high (~95%), which is in agreement with previous observations (Mathivet *et al.,* 1996; Bagatolli and Gratton, 1999, 2000a, 2000b). After the vesicles were formed, the AC field was turned off and the experiments were carried out at room temperature. Using this methodology, single vesicles (adsorbed to the Pt wire) can be observed for relatively long times (these types of vesicles are usually stable for more than 8 hr).

2.4. GUVs: LAURDAN Labeling and GP Determinations

Generalized polarization (GP) is defined as follows:

$$GP = (I_B - I_R)/(I_B + I_R)$$

where I_B and I_R are the intensities in the blue and red edges of an emission spectrum, respectively, using a given excitation wavelength (Parasassi *et al.,* 1990, 1991). This function allows quantification of the spectral changes in the emission of a fluorophore as a consequence of environmental perturbation.

The amphiphilic LAURDAN molecule partitions strongly into lipid phases (Parasassi *et al.,* 1990, 1991). When associated with phospholipid vesicles, the fluorescent moiety of LAURDAN is located at the glycerol backbone region of the bilayers (Parasassi and Gratton, 1995; Parasassi *et al.,* 1998; Bagatolli *et al.,* 1999). The emission spectrum of LAURDAN shows a continuous shift from blue to green during the main lipid phase transition, namely, gel phase to fluid phase (Parasassi and Gratton, 1995; Parasassi *et al.,* 1998; Bagatolli *et al.,* 1999). In the lipid gel phase, the emission spectrum of LAURDAN has a maximum at 440 nm; in the fluid phase the maximum is at 490 nm (Parasassi *et al.,* 1990, 1991). This dramatic spectral shift has been attributed to dipolar relaxation due to reorientation of water molecules around the excited state dipole of LAURDAN. As a consequence, the GP function for LAURDAN is sensitive to the phase state of the lipid, which determines the extent of water penetration; that is, the more fluid the bilayer, the more water is present near the excited fluorophore (Parasassi and Gratton, 1995; Parasassi *et al.,* 1998; Bagatolli *et al.,* 1999). One way to depict GP values in GUVs is to present a GP histogram (Bagatolli and Gratton, 2000a, 2000b; Dietrich *et al.,* 2001) in which the GP value of each pixel is

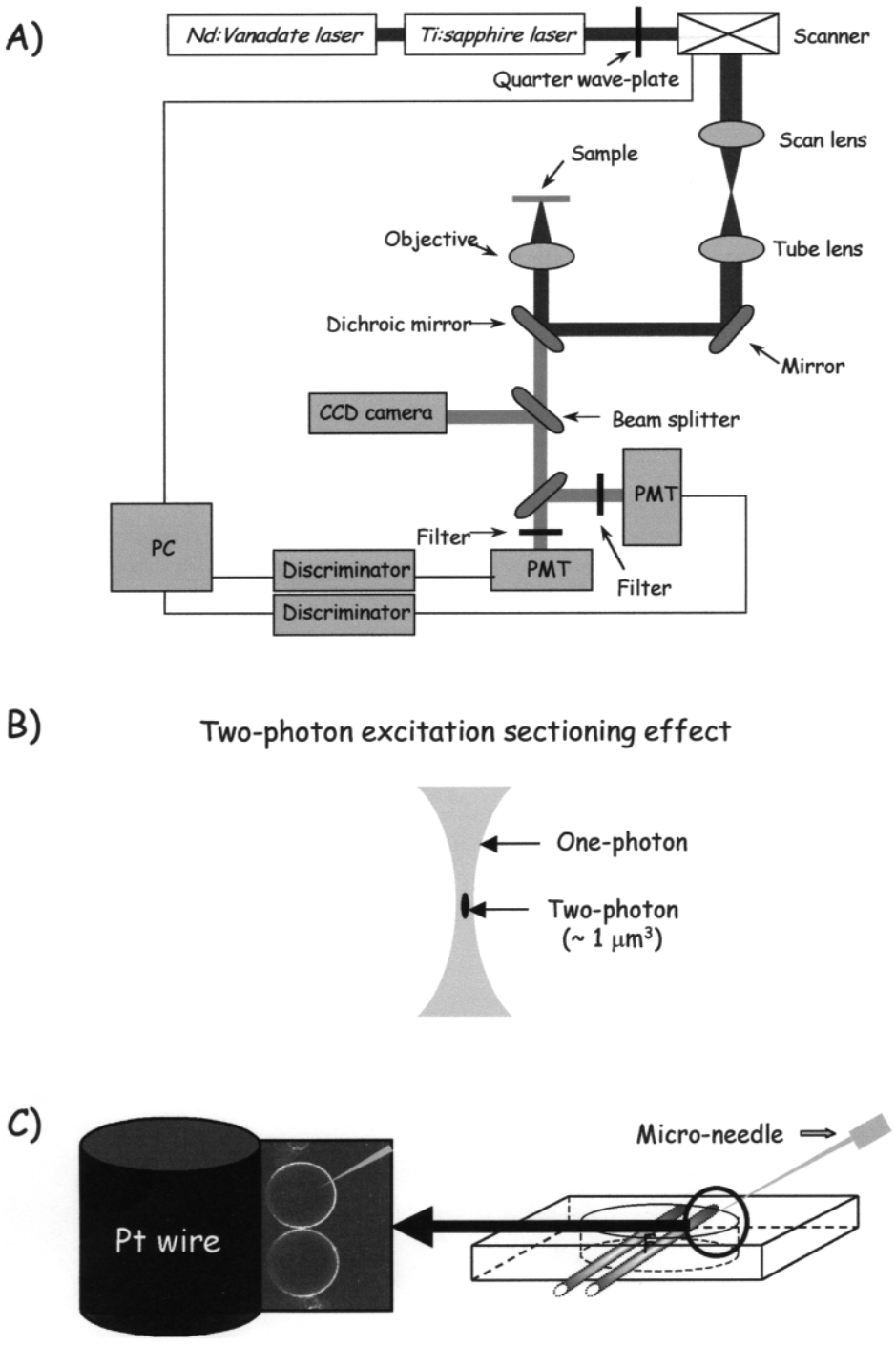

Fig. 2. Schematic diagram of the two-photon microscope setup (A), two-photon sectioning effect (B), and GUV formation chamber (C).

determined and then used to construct a plot of fraction of pixels with a given GP value versus the GP value.

For the LAURDAN experiments, vesicles were labeled as described previously (Bagatolli and Gratton, 1999, 2000a, 2000b). Briefly, ~1 μl of a LAURDAN/dimethyl sulfoxide stock solution was added to the chamber after vesicle formation. Typically, a final LAURDAN/lipid ratio of 1:500 mol/mol was obtained. The GP function was calculated as previously reported (Parasassi *et al.*, 1997; Bagatolli and Gratton, 1999, 2000a, 2000b). Briefly, two images of the same LAURDAN-labeled GUV were obtained simultaneously using two optical bandpass filters (Ealing Electro-optics, Holliston, MA) with 46 nm bandwidth and centers at 446 nm (I_B) and 499 nm (I_R). Subsequently, the two intensity images corresponding to the different filters were processed to calculate the GP image.

2.5. Addition of Dynamin II to GUVs

In all these experiments, a particular GUV was selected and centered in the two-photon excitation scanning area. Next, a 0.5-μm-diameter microneedle was placed within ~5 μm of the target GUV and dynamin II (labeled or unlabeled dynamin; ~20 μM stock solution) was added using a microinjector. The typical addition volume was 65 femptoliters. Before the protein experiments, buffer alone was injected close to the GUVs to evaluate the possible effects of the change in the local ionic strength on the structure and stability of the GUVs. In these control experiments, no changes in GUV structure were observed.

2.6. Two-Photon Fluorescence Microscopy

The scanning two-photon fluorescence microscope has been described in detail elsewhere (So *et al.*, 1995, 1996). A schematic of this instrument is shown in Fig. 2. Briefly, the two-photon excitation source is a titanium–sapphire laser (Mira 900; Coherent Palo Alto, CA) pumped by a frequency-doubled neodymium–vanadate laser (Verdi; Coherent). Scanning in both the *x* and *y* directions was achieved using a galvanometer-driven scanner (Cambridge Technology, Watertown, MA) controlled by a frequency synthesizer (Hewlett-Packard, Santa Clara, CA). A 20-s frame rate was used to acquire the images (256 × 256 pixels). We used a long working distance air objective (Zeiss 20X LD-Achroplan, 0.4 N.A.) The pixel size was determined using fluorescent label latex spheres (14.4-μm diameter) and corresponds to 0.52 μm.

3. RESULTS

Figure 3 shows the images obtained after addition of fluorescein-labeled dynamin II to GUVs composed of POPC/PI(4,5)P_2 10:1 mol/mol. These images, which

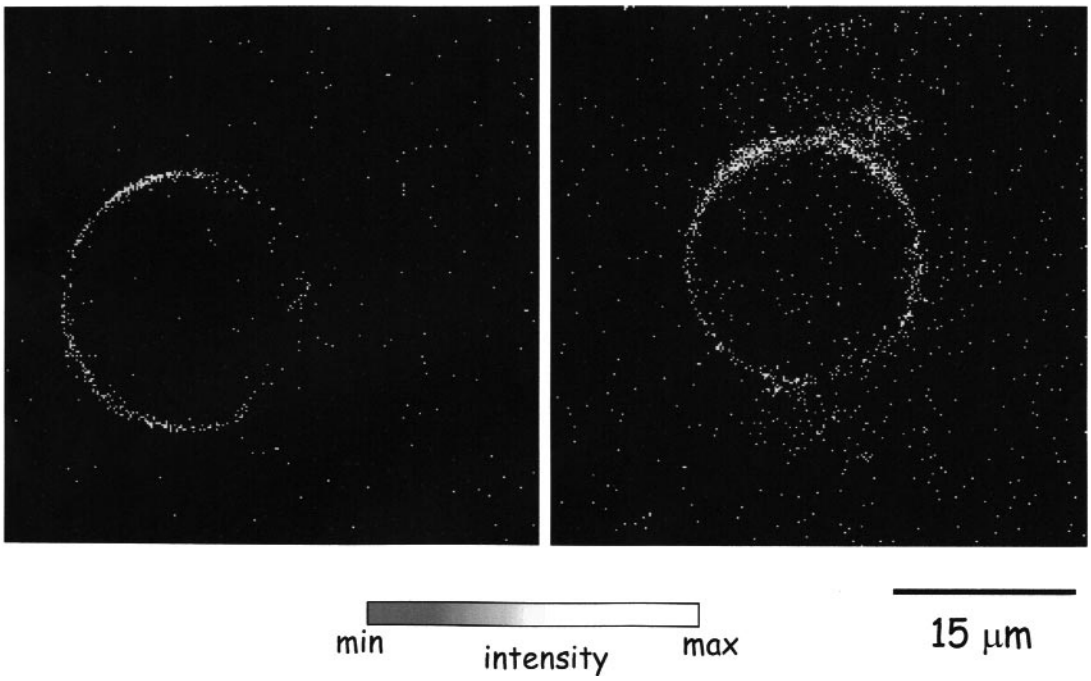

Fig. 3. Binding of fluorescein-labeled dynamin II to GUVs composed of POPC/PI(4,5)P_2 ratio of 10:1 mol/mol.

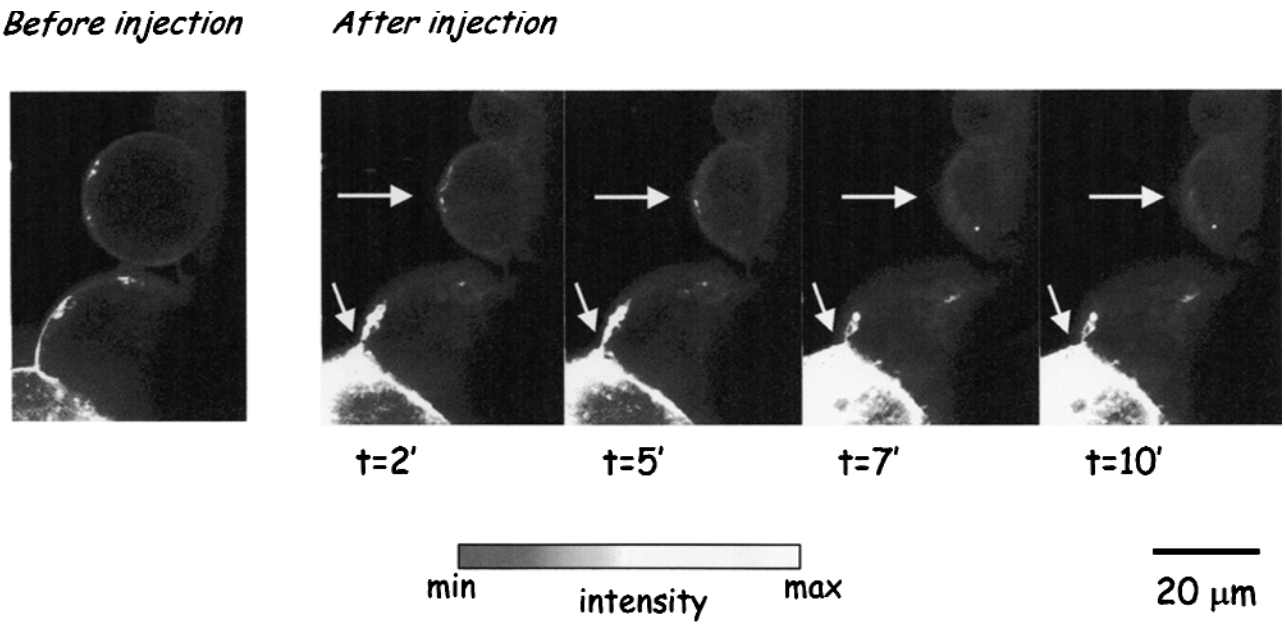

Fig. 4. Time course of the effect of dynamin II on LAURDAN-labeled GUVs (POPC/PI(4,5)P_2 ratio of 10:1 mol/mol) before and after addition of unlabeled dynamin II. Cross-sections close to the top part of the GUV were observed.

correspond to cross-sections through the center of two different GUVs, clearly show fluorescence restricted to the membrane border. Furthermore, the protein distribution on the membrane is not uniform and appears to show patches of fluorescence in some areas on the vesicle surface. Figure 4 shows a time sequence of LAURDAN-labeled GUVs (POPC/PI(4,5)P_2 10:1 mol/mol) before and after addition of unlabeled dynamin II. In this case, cross-sections close to the top part of the GUV were observed. An increase in fluorescence intensity with time, near the junction of two vesicles, is apparent.

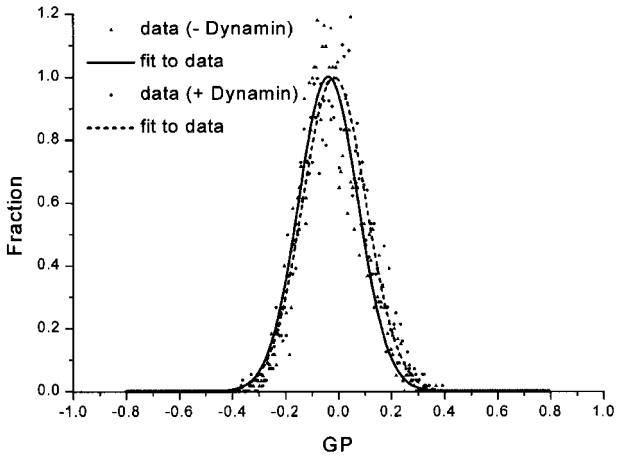

Fig. 5. LAURDAN GP histograms calculated for GUVs in the absence and presence of dynamin.

To evaluate the effect of addition of dynamin II on the physical state of the lipid in the GUVs, the GP of LAURDAN was calculated before and after addition of protein. As shown in Fig. 5, the resulting GP histograms were essentially identical. Figure 6 shows the fluorescence due to mant-GTPγS, in the presence of GUVs, before and after addition of unlabeled dynamin II. As can be seen in these images, the GUV border is not apparent until dynamin II is present. Figure 7 shows GUV images from two different experiments on GUVs formed from pure POPC (i.e., in the absence of PI(4,5)P_2), namely, addition of unlabeled dynamin II in the presence of mant-GTPγS (panel A) and addition of fluorescein-labeled dynamin II (panel B). The effects of POPC on the GTPase activities of both dynamin I and II are shown in Fig. 8. These data clearly demonstrate that these two dynamin isoforms respond differently to POPC. The effect of pure POPC on the GTPase activity of dynamin II was then studied in more detail, as shown in Fig. 9. As can be seen, the GTPase activity is potently stimulated by POPC vesicles; half-maximal activation occurs at ~10 μM phospholipid.

4. DISCUSSION

Two-photon microscopy was used to monitor binding of the GTPase dynamin II to GUVs. Although dynamin II is known to interact with various lipids, the images presented in Fig. 3 are the first to directly visualize

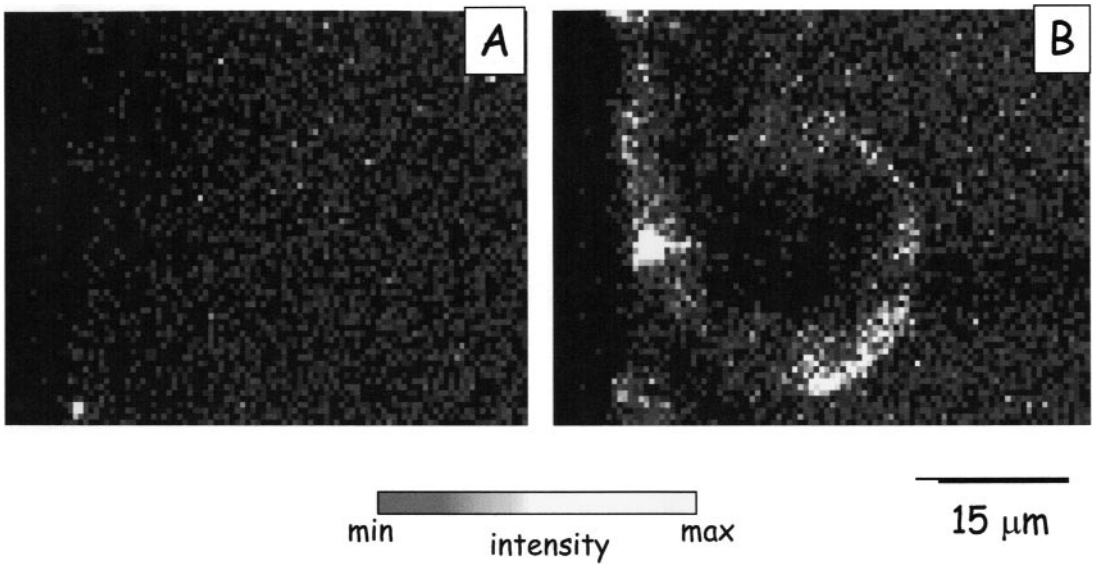

Fig. 6. Two-photon images of a field containing a GUV (POPC/PI(4,5)P_2 ratio of 10:1 mol/mol) in the presence of mant-GTPγS before (A) and after (B) addition of unlabeled dynamin.

the binding of dynamin II to vesicles. The images shown in Fig. 4 also clearly indicate that dynamin II affects the vesicle morphology and the overall distribution of the LAURDAN. Specifically, the results shown in Fig. 4 suggest that dynamin II binding to vesicles produces an increase in the amount of LAURDAN-labeled lipid material in the scanned region, which increases the fluorescence intensity (note that the LAURDAN was homogeneously distributed before addition of protein). The fact that the GP histogram does not change after the addition of dynamin II indicates that the physical state of the lipid phase is not significantly altered.

Previous studies using large unilamellar vesicles have shown that anionic lipids are required for the dynamin-induced vesicularization in the presence of GTP (Sweitzer and Hinshaw, 1998; Takei *et al.*, 1998). Hence, an unsuspected finding of the present work was the interaction between dynamin II and GUVs composed solely of

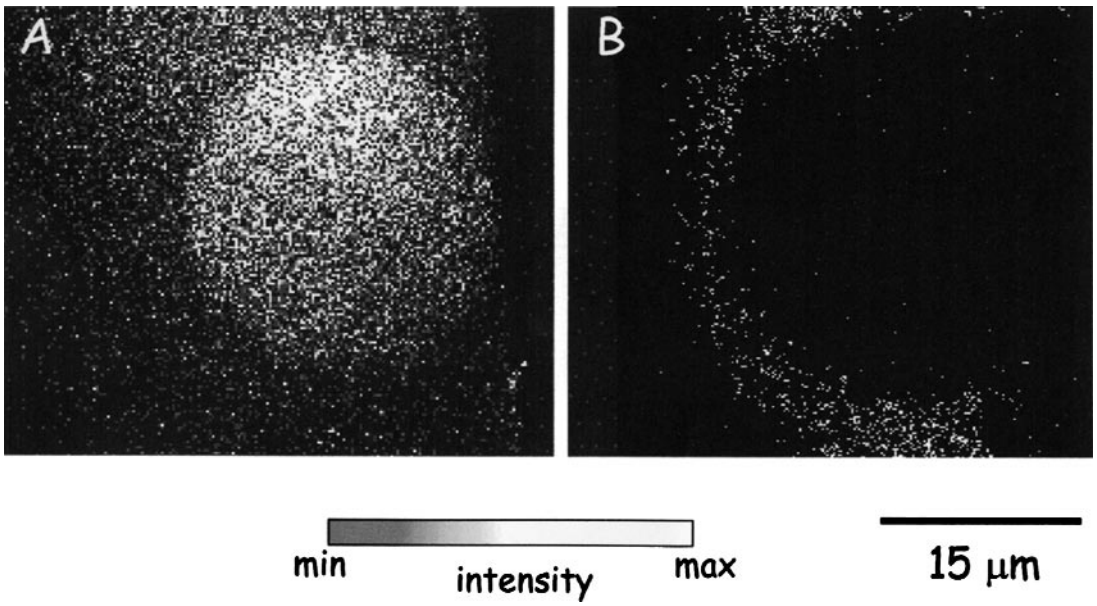

Fig. 7. Binding of dynamin II to GUVs formed from pure POPC (i.e., in the absence of PI(4,5)P_2). A, Top view of a GUV with unlabeled dynamin in the presence of mant-GTPγS. B, Cross-section of GUV with fluorescein-labeled dynamin.

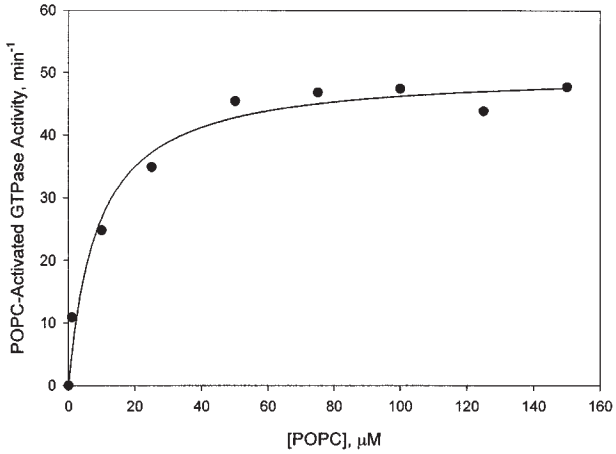

Fig. 8. Effect of POPC on activation of dynamin I and II (37°C).

the neutral lipid POPC. Earlier reports from our laboratory (Barylko *et al.,* 1998) and others (Salim *et al.,* 1996; Tuma *et al.,* 1993; Zheng *et al.,* 1996) showed that the neural-specific form of dynamin—dynamin I—binds only to liposomes containing negatively charged lipids, which stimulate its GTPase activity. It was further shown that both dynamin I and the ubiquitously expressed dynamin II interact with phosphoinositides by virtue of their PH domains (Achiriloaie *et al.,* 1999; Salim *et al.,* 1996; Zheng *et al.,* 1996) and that this interaction is critical for the ability of dynamin to promote endocytosis in cells (Vallis *et al.,* 1999; Archiroloaie *et al.,* 1999). Here we confirmed that the GTPase activity of dynamin I is unaffected by POPC liposomes, whereas dynamin II GTPase activity is stimulated nearly twofold. It should be noted that dynamin I, which has a 10-fold lower basal activity than dynamin II, is stimulated to $\sim$200 min^{-1} by PIP_2.

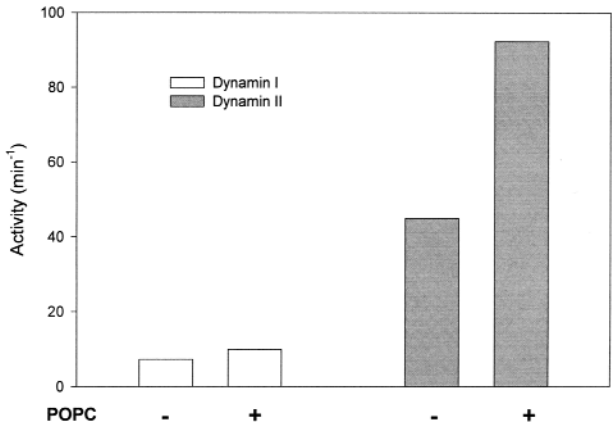

Fig. 9. GTPase activation of dynamins I and II by POPC vesicles. Dynamin concentrations were 0.1 μM (37°C).

The region within dynamin II that is responsible for interacting with POPC vesicles has yet to be identified. Based on data showing a direct interaction between the phospholipase C-β PH domain and neutral lipids (Wang *et al.,* 1999), the dynamin II PH domain is a likely binding determinant. If so, the specific activation of dynamin II by POPC may seem surprising, in view of the 84% sequence similarity (76% sequence identity) between the PH domains of the two dynamin isoforms. However, functional differences between dynamin I and II PH domains have already been shown. For example, the introduction of dynamin I PH domain into adrenal chromaffin cells blocks membrane retrieval after exocytosis, whereas introduction of the dynamin 2 PH domain has no effect (Artalejo *et al.,* 1997). Conversely, overexpression of the dynamin II PH domain inhibits Golgi budding but is unaffected by expression of the dynamin I PH domain (Yang *et al.,* 2001). These specific properties cannot be explained by differences in affinities to phosphoinositides, because the two PH domains bind equally well to these lipids (Klein *et al.,* 1998).

Finally, we have shown that the use of two-photon fluorescence microscopy coupled with GUV methodologies can be used to study dynamin-lipid interactions. Present efforts are being directed toward developing an assay for the vesicluarization activity of dynamin based on these methodologies.

ACKNOWLEDGMENTS

This research was supported by National Institutes of Health (NIH) grant GM555620 (J.P.A.), American Heart Association grant 9950020N (D.M.J.), and Fundación Antorchas, Argentina (L.A.B). L.A.B. is a member of the CONICET (Argentina) Investigator Career. The two-photon excitation microscopy experiments were performed at the Laboratory for Fluorescence Dynamics (NIH grant RR03155), Department of Physics, University of Illinois at Urbana-Champaign.

REFERENCES

Angelova, M. I., Soléau, S., Meléard, Ph., Faucon, J. F., and Bothorel, P. (1992). *Progr. Colloid Polym. Sci.* **89:** 127–131.
Artalejo, C. R., Lemmon, M. A., Schlessinger, J., and Palfrey, H. C. (1997). *EMBO J.* **16:** 1565–1574.
Bagatolli, L. A., and Gratton, E. (1999). *Biophys. J.* **77:** 2090–2101.
Bagatolli, L. A., and Gratton, E. (2000a). *Biophys. J.* **78:** 290–305.
Bagatolli, L. A., and Gratton, E. (2000b). *Biophys. J.* **79:** 434–447.
Bagatolli, L. A., and Gratton, E. (2001). *J. Fluorescence* **11:** 141–160.
Bagatolli, L. A., Gratton, E., Khan, T. K., and Chong, P. L. G. (2000). *Biophys. J.* **79:** 416–425.

Bagatolli, L. A., Parasassi, T., Fidelio, G. D., and Gratton, E. (1999). *Photochem. Photobiol.* **70:** 557–564.
Barylko, B., Bennes, D., Lim, K.-M., Atkinson, M. A. L., Jameson, D. M., Yin, H. L., *et al.* (1998). *J. Biol. Chem.* **273:** 3791–3797.
Binns, D. D., Barylko, B., Grichine, N., Atkinson, M. A. L., Helms, M. K., Jameson, D. M., *et al.* (1999). *J. Prot. Chem.* **18:** 277–290.
Binns, D. D., Helms, M. K., Barylko, B., Davis, C. T., Jameson, D. M., Albanesi, J. T., *et al.* (2000). *Biochemistry* **39:** 7188–7196.
Cao, H., Garcia, F., and McNiven, M. A. (1998). *Mol. Biol. Cell* **9:** 2595–2609.
Chen, M. S., Obar, R. A., Schroeder, C. C., Austin, T. W., Poodry, C. A., Wadsworth, S. C., *et al.* (1991). *Nature* **351:** 583–586.
Cook, T. A., Urrita, R., and McNiven, M. A. (1994). *Proc. Natl. Acad. Sci. USA* **91:** 644–648.
Dietrich, C., Bagatolli, L. A., Volovyk, Z., Thompson, N. L., Levi, M., Jacobson, K., *et al.* (2001). *Biophys. J.* **80:** 1417–1428.
Gennis, R. B. (1989). *Biomembranes*, Springer-Verlag, Heidelberg.
Hiratsuka, T. (1983). *Biochim. Biophys. Acta* **742:** 496–508.
Henley, J. R., Krueger, E. W., Oswald, B. J., and McNiven, M. A. (1998). *J. Cell Biol.* **141:** 85–99.
Herskovits, J. S., Burgess, C. C., Obar, R. A., and Vallee, R. B. (1993). *J. Cell Biol.* **122:** 565–578.
Hinshaw, J. E. (1999). *Curr. Opin. Struct. Biol.* **9:** 260–267.
Jameson, D. M., and Eccleston, J. F. (1997). *Meth. Enzymol.* **278:** 363–390.
Jones, S. M., Howell, K. E., Henley, J. R., Cao, H., and McNiven, M. A. (1998). *Science* **279:** 573–577.
Klein, D. E., Lee, A., Frank, D. W., Marks, M. S., and Lemmon, M. A. (1998). *J. Biol. Chem.* **273:** 27725–27733.
Lin, H. C., Barylko, B., Achiriloaie, M., and Albanesi, J. P. (1997). *J. Biol. Chem.* **272:** 25999–26004.
Mathivet, L., Cribier, S., and Devaux, P. F. (1996). *Biophys. J.* **70:** 1112–1121.
McNiven, M. A. (1998). *Cell* **94:** 151–154.
McNiven, M. A., Cao, H., Pitts, K. R., and Yoon, Y. (2000). *Trends Biochem. Sci.* **25:** 115–120.
McPherson, P. S. (1999). *Cell. Signal.* **11:** 229–238.
Muhlberg, A. B., Warnock, D. E., and Schmid, S. L. (1997). *EMBO J.* **16:** 6676–6683.
Nakata, T., Takemura, T., and Hirokawa, N. (1993). *J. Cell Sci.* **105:** 1–5.
Obar, R. A., Collins, C. A., Hammerback, J. A., Shpetner, H. S., and Vallee, R. B. (1990). *Nature* **347:** 256–261.
Oh, P., McIntosh, D. P., and Schnitzer, J. E. (1998). *J. Cell Biol.* **141:** 101–114.
Okamoto, P. M., Herskovits, J. S., and Vallee, R. B. (1997). *J. Biol. Chem.* **272:** 11629–11635.
Parasassi, T., De Stasio, G., d'Ubaldo, A., and Gratton, E. (1990). *Biophys. J.* **57:** 1179–1186.
Parasassi, T., De Stasio, G., Ravagnan, G., Rusch, R. M., and Gratton, E. (1991). *Biophys. J.* **60:** 179–189.
Parasassi, T., and Gratton, E. (1995). *J. Fluorescence* **5:** 59–70.
Parasassi, T., Gratton, E., Yu, W., Wilson, P., and Levi, M. (1997). *Biophys. J.* **72:** 2413–2429.
Parasassi, T., Krasnowska, E., Bagatolli, L. A., and Gratton, E. (1998). *J. Fluorescence* **8:** 365–373.
Remmers, A. E. (1998). *Anal. Biochem.* **257:** 89–94.
Salim, K., Bottomley, M. J., Querfurth, E., Zvelebil, M. J., Gout, I., Scaife, R., *et al.* (1996). *EMBO J.* **15:** 6241–6250.
Schmid, S. L., McNiven, M. A., and De Camilli, P. (1998). *Curr. Opin. Cell Biol.* **10:** 504–512.
Shpetner, H. S., and Vallee, R. B. (1992). *Nature* **355:** 733–735.
Shpetner, H. S., Herskovits, J. S., and Vallee, R. B. (1996). *J. Biol. Chem.* **271:** 13–16.
So, P. T. C., French, T., Yu, W. M., Berland, K. M., Dong, C. Y., and Gratton, E. (1995). *Bioimaging* **3:** 49–63.
So, P. T. C., French, T., Yu, W. M., Berland, K. M., Dong, C. Y., and Gratton, E. (1996). In: Wang, X. F., and Herman, B. (eds.), *Chemical Analysis Series* (Vol. 137), John Wiley and Sons, New York, pp. 351–374.
Sontag, J.-M., Fyske, E. M., Ushkaryov, Y., Liu, J.-P., Robinson, P. J., and Sudhof, T. C. (1994). *J. Biol. Chem.* **269:** 4547–4554.
Sweitzer, S. M., and Hinshaw, J. E. (1998). *Cell* **93:** 1021–1029.
Takei, K., Haucke, V., Slepnev, V., Farsad, K., Salazar, M., Chen, H., *et al.* (1998). *Cell* **94:** 131–141.
Tuma, P. L., Stachniak, M. C., and Collins, C. A. (1993). *J. Biol. Chem.* **268:** 17240–17246.
van der Bliek, A. M. (1999a). *Trends Cell Biol.* **9:** 96–102.
van der Bliek, A. M. (1999b). *Trends Cell Biol.* **9:** 253–254.
van der Bliek, A. M., Redeimeisner, T. E., Damke, H., Tisdale, E. J., Meyerowitz, E. M., and Schmid, S. L. (1993). *J. Cell Biol.* **12:** 553–563.
Wang, T., Pentyala, S., Rebecchi, M. J., and Scarlata, S. (1999). *Biochemistry* **38:** 1517–1524.
Yang, Z., Li, H., Chai, Z., Fullerton, M. J., Cao, Y., Toh, B. H., *et al.* (2001). *J. Biol. Chem.* **276:** 4251–4260.
Yu, W., So, P. T., French, T., and Gratton, E. (1996). *Biophys. J.* **70:** 626–636.
Zheng, J., Cahill, S. M., Lemmon, M. A., Fushman, D., Schlessinger, J., and Cowburn, D. (1996). *J. Mol. Biol.* **255:** 14–21.